Energy Transfer from Photo-Excited Fluorene Polymers to Single-Walled Carbon Nanotubes

ARTICLE *in* THE JOURNAL OF PHYSICAL CHEMISTRY C · AUGUST 2009

Impact Factor: 4.77 · DOI: 10.1021/jp904431u

Energy Transfer from Photo-Excited Fluorene Polymers to Single-Walled Carbon Nanotubes

FuMing Chen,[†] Wenjing Zhang,[†] Mingli Jia,[‡] Li Wei,[§] Xiao-Feng Fan,[||] Jer-Lai Kuo,[||] Yuan Chen,[§] Mary B. Chan-Park,[§] Andong Xia,[‡] and Lain-Jong Li*[,†]

School of Materials Science and Engineering, Nanyang Technological University, 50 Nanyang Ave., Singapore 639798, The State Key Laboratory of Molecular Reaction Dynamics Institute of Chemistry, Chinese Academy of Sciences, Beijing 100080, P.R. China, School of Chemical and Biomedical Engineering, Nanyang Technological University, Singapore 637459, and School of Physical and Mathematical Sciences, Nanyang Technological University, Singapore 637371

Received: May 12, 2009

The energy transfer from fluorene-based polymers such as poly(9,9-dioctylfluoreny-2,7-diyl) (PFO) and poly[(9,9-dioctylfluorenyl-2,7-diyl)-*co*-(bithiophene)] (F8T2) to single-walled carbon nanotubes (SWNTs) is proved by photoluminescence excitation (PLE) and fluorescence lifetime studies. The excitation wavelength to cause optimal emissions from SWNTs is tunable in a wide wavelength range from 388 to 480 nm (from 488 to 520 nm) depending on the concentration of excess PFO (F8T2) polymers. The energy transfer and hence the excitation wavelength to cause optimal SWNT emissions is govern by the chain conformation and aggregation state of the polymers proximate to SWNT surfaces. The PLE mapping technique, an ideal method to monitor the energy transfer process, is adopted to study the SWNT binding competition between PFO and F8T2. We conclude that SWNTs are preferentially bound with F8T2 polymers. Moreover, the molecular dynamic simulation also agrees well with the experiment results. This study explores the photon conversion process between aromatic polymers and SWNTs and suggests a convenient method of adjusting the desired wavelength for the optimal energy conversion, useful for polymer-SWNT composites in optoelectronic applications.

Introduction

The conversion of sunlight to chemical energy has become an increasingly compelling problem and drawn considerable attention.[1] Incorporation of single-walled carbon nanotubes (SWNTs) into a conducting polymer for organic photovoltaic applications has recently been demonstrated.[2] Photon absorption in aromatic polymers produces bound-state electron−hole pairs, known as excitons. These electron−hole pairs can radiatively recombine and emit photons, which is called photoluminescence (PL). The addition of semiconducting SWNTs has been shown to induce the transfer of holes or electrons to the nanotubes depending on the electronic energy alignment between the SWNTs and polymers.[3−7] Thus this process may be adopted for applications in photodetectors based on chromophore−SWNT composites.[7−9] Since the first observation of photoluminescence from surfactant-dispersed SWNTs in solution,[10] researchers have realized that the optically excited electronic states of SWNTs are highly mobile and sensitive to the surrounding surfactants or solvents.[11−13] Photoactive aromatic polymers have also been used to disperse SWNTs for spectroscopic studies.[14−20] In particular, the photon-generated excitons in aromatic polymers are also likely to be transferred from polymers to SWNTs, resulting in near-infrared (NIR) photoemission from the semiconducting SWNTs. Recent studies[14,15] have proposed the possibility of energy transfer from polymer to SWNTs. We noticed that the concentration of the polymer used in these reports was relatively high. And also it appears that the observed excitation wavelength for causing optimal energy transfer from polymers to SWNTs (optimal excitation wavelength) was longer than the expected peak energy of polymer absorption. These interesting experimental observations could indicate that the polymer π-conjugation chain governing the energy transfer in the polymer−SWNT system is relatively more extended compared with that for the pure polymer system. Thus, the energy transfer process is still not well-understood and worth detailed investigations. Also, the fundamental understanding of the optical behaviors of the aromatic polymer−SWNT composite is crucial for their optoelectronic applications.

Herein, we carefully study the effect of polymer concentration on the energy transfer process from fluorene-based polymers to SWNTs and demonstrate that the optimal excitation wavelength is polymer-concentration dependent; the wavelength can be tuned in a wide range from 388 nm up to 480 nm for poly(9,9-dioctylfluoreny- 2,7-diyl) (PFO) and from 480 nm to 520 nm for poly[(9,9-dioctylfluorenyl-2,7-diyl)-co-(bithiophene)] (F8T2). We interpret this due to the control of extended π-conjugation in the polymers close to SWNT surfaces. This study suggests a simple way of tuning optimal excitation wavelength without changing the chemical functionality of the polymers. Moreover, the PLE mapping techniques are successfully used to study the SWNT binding competition between F8T2 and PFO polymers.

* To whom correspondence should be addressed. E-mail: ljli@ntu.edu.sg.
[†] School of Materials Science and Engineering, Nanyang Technological University.
[‡] Chinese Academy of Sciences.
[§] School of Chemical and Biomedical Engineering, Nanyang Technological University.
[||] School of Physical and Mathematical Sciences, Nanyang Technological University.

10.1021/jp904431u CCC: $40.75
Published on Web 07/01/2009

Experimental Section

Sample Preparations. PFO and F8T2 were from American Dye Source and CoMoCat SWNTs were from SouthWest NanoTechnologies. The preparation of the polymer−SWNT dispersion in toluene has been reported elsewhere.[15,16,21] In brief, SWNT powders were dispersed in polymer/toluene solutions in the ratio 8 mg of SWNT:10 mg of polymer:80 mL of solvent. The solutions were then homogenized in a sonic bath for 30 min followed by probe sonication for 45 min. It was then promptly followed by centrifugation at 14200 g for 30 min. The supernatant was filtered with Teflon filter papers (200 nm pore size). The recovered precipitates were thoroughly washed with toluene until the characteristic absorption band from the free polymer completely disappeared in toluene.

The preparation of polymer−SWNT solutions for optical measurements is described using PFO-SWNT as an example: 0.05 mg of washed precipitated PFO-SWNT hybrid obtained on the filter paper, reckoned to contain low amounts of PFO, was then redispersed into 4 mL of toluene, and we named this PFO-SWNT solution as PFO-SWNT(0). The concentration of PFO and SWNT in this hybrid, PFO-SWNT(0), $\sim 3.7 \times 10^{-4}$ and $\sim 1.79 \times 10^{-4}$ mg/mL respectively, was estimated from their absorbance. (Supporting Information, Figure S1). A solution with higher amounts of excess PFO polymers, PFO-SWNT(0)+PFO, was then prepared by adding desired amounts of excess PFO to the PFO-SWNT(0) solution. Similarly, the F8T2-SWNT solutions with excess F8T2 were prepared by adding desired amounts of F8T2 polymers to the F8T2-SWNT(0) solution.

PLE and Fluorescence Lifetime Measurements. Photoluminescence excitation (PLE) mapping was performed with a Jobin-Yvon Horiba Fluorolog-3 spectrophotometer. Fluorescence lifetimes were measured by standard time-correlated single-photon counting (TCSPC) from Ortac at room temperature. The excitation source was a titanium sapphire laser (Coherent Mira 900) with 200 fs pulse duration operated at 76 MHz. The fundamental beam was sent through a pulse picker (coherent 9200) and a second harmonic generation (SHG) crystal to obtain the 380 and 440 nm laser pulses at 4.7 MHz for excitations of PFO and F8T2, respectively. Fluorescence was detected by using a monochromator (EI-121, Edinburgh Instruments) and fast photomultiplier tube (XP2020). The instrument response function (IRF) measured by scattering the excitation light from a dilute suspension of colloidal silica was about 220 ps to provide ~50 ps time resolution with deconvolution. All of the temporal evolution profiles are fitted by the convolution between the IRF with a monoexponential function according to iterative deconvolution by FluoFit software based on the Levenberg−Marquardt and Simplex algorithms (Version 3.3, PicoQuant, Germany).

Molecular Simulation. Molecular adsorptions of F8T2 and PFO on SWNT with chirality (7, 5) were investigated with Forcite program within the Materials Studio software environment.[22] Molecular systems were constructed and visualized with Materials Studio, and Universal force field (UFF)[23] was adapted to describe the molecular interactions. To explore the stable conformation of the polymers adsorbed on SWNT, we engaged a series of molecular dynamics (MD) simulations with NVE ensemble at about 310 K. Different configurations, along the long MD trajectories, were selected and quenched to yield the most stable conformations between the aromatic polymers and SWNT. To allow the system to explore different conformations, we did not use periodic boundary condition, and therefore, SWNTs are terminated by hydrogen atoms.

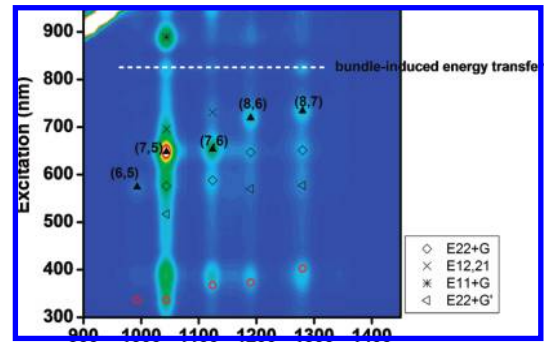

Figure 1. PLE map of PFO-SWNT(0). Five major species (6,5), (7,5), (7,6), (8,6), and (8,7) are noted. Excitation satellites from either bundled tubes or from phonon-assisted emission ($E_{22} + G$, $E_{12,21}$, $E_{11} + G$, $E_{22} + G'$) are also indicated. Empty circles represent the E_{11} emissions of SWNTs through their E_{33} excitation.

Results and Discussion

Fluorene-based polymers have been used to selectively disperse SWNTs in organic solvents; the PL spectra of such suspensions are relatively simple (with fewer species) and the PL peaks are of narrow width. Moreover, the phonon−exciton interactions as well as the relaxation of the photoexcited carriers in PFO-wrapped SWNTs have been carefully studied.[24,25] Therefore PFO is used to study the energy transfer to SWNTs. Due to that the CoMoCat SWNTs are with relatively fewer species compared with other sources of SWNTs, we mainly focused on this type of tubes to allow better identification of the features in PLE mappings.

Assignment of Features in PLE Mapping. Figure 1 shows the PLE mapping for PFO−SWNT(0) in toluene. We monitor the near-infrared (NIR) emissions from various SWNT species by excitation with a wide-range of wavelengths (300−900 nm), covering from UV to NIR. Based on the emission wavelength from first van Hove band gap (E_{11}) and the resonance excitation wavelength of their second van Hove band gaps (E_{22}), five major SWNT chiral species (6,5), (7,5), (7,6), (8,6), and (8,7) are identified in Figure 1. Excitation satellites from either bundled tubes[26] or from phonon-assisted emission[24,25] are also indicated and described below. Following Lebedkin's work,[24] we attribute most of the satellite peaks to phonon-coupled photoexcitations, such as ($E_{11} + G$), ($E_{22} + G$), ($E_{22} + G'$), and transverse photoexcitation ($E_{12,21}$), as indicated in Figure 1. The excitation at 822 nm results in the emission from all species; this is attributed to exciton energy transfer from bundled tubes. Based on Tan's work,[26] it is likely that the (5,4) tubes form nanotube bundles with other species and that the 822 nm excitation directly generates the exciton through the E_{11} gap in (5,4) tubes, and the excitons subsequently transfer to other species. Also, the empty circles represent the E_{11} emissions of SWNTs excited through their third van Hove gap energy (E_{33}). In fact, we are more concerning about the SWNT emissions when the excitation is at ~388 nm because these emissions are caused by the energy transfer from PFO to SWNTs, which will be discussed in Figure 2b.

Energy Transfer from PFO to SWNTs. Now we discuss the PLE mappings for the PFO-SWNT hybrid with various amounts of excess PFO polymers in toluene. We compare the PLE mapping for PFO-SWNT(0) and PFO-SWNT(0)+PFO (0.5 mg/mL) in Figure 2, panels b and c. Interestingly, for the PFO-SWNT(0) in Figure 2b, we observe emission from all present species when the excitation wavelength is around 388 nm, which is in coincidence with the maximum absorption wavelength (~386 nm) of the PFO polymer as shown in Figure 2d. These

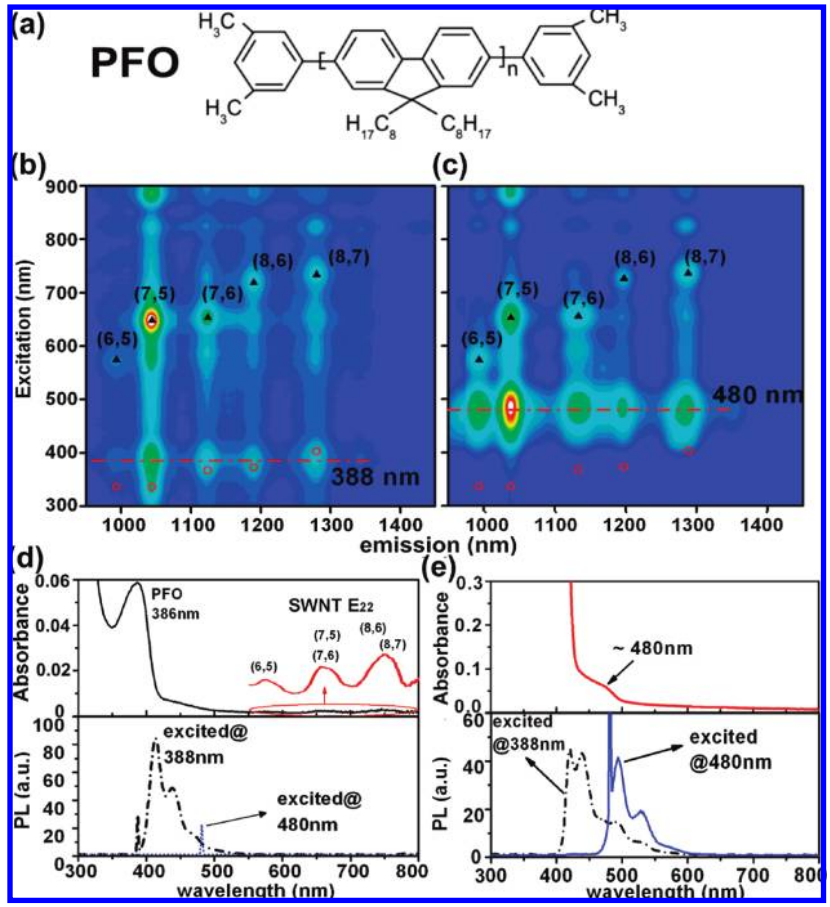

Figure 2. (a) Chemical structure of PFO. PLE mappings for (b) PFO-SWNT(0), and (c) PFO-SWNT(0)+PFO (0.5 mg/mL). Typical optical absorption and PL spectra (excited @388 and 480 nm) for the solutions of (d) PFO-SWNT (0), and (e) PFO-SWNT(0)+PFO (0.5 mg/mL). It is noted that the absorbance of PFO in 1(e) is out of scale due to the high PFO concentration.

emissions are unlikely resulted from the E_{33} resonance excitation owing to the mismatch of the PLE peak positions. The emission peaks due to E_{33} resonance excitation[27,28] for the SWNT species are also indicated as empty circles in Figure 2, panels b and c for clarifications. We have also verified that the excitation at 388 nm does not cause NIR emissions for the SWNTs dispersed in a commonly used surfactant, sodium dodecylsulfate (data not shown). These results suggest that the PFO polymers function as a light absorber which may transfer energy to SWNTs and cause NIR emissions of SWNTs subsequently. We notice that the PFO emission exhibits a long tail extending to a longer wavelength (Figure 4d), which may contribute to the energy transfer. Also, the electron density-of-state in SWNTs is nonzero beyond the first van Hove singularities and therefore the weak absorption between E_{22} and E_{33} peaks could contribute to the energy transfer as well.

Figure 2c shows the PLE map for the PFO-SWNT solution added with a large quantity (0.5 mg/mL) of excess PFO polymers, the optimal excitation wavelength for SWNT emissions (through energy transfer) is drastically shifted to 480 nm. Also, we notice that the excitation at the major PFO absorption peak (388 nm) for this solution does not cause obvious NIR emissions from SWNTs by contrast to that observed in Figure 2c. Instead, the excitation at 388 nm only results in strong visible emissions from PFO itself (Figure 2e). It is generally believed at least two types of PFO polymers are present in concentrated PFO solution: (1) free or nearly free polymers which exhibit an absorption peak at ~388 nm and (2) aggregated β-phase polymers with an absorption peak centered at 437 nm.[29,30] The unpronounced SWNT emission at 388 nm excitation in Figure 2c suggests that the energy transfer process from free polymer to SWNTs is not efficient in the presence of excess PFO. Also, the excitation at 437 nm does not cause the optimal SWNT emissions as shown in Figure 2c. Thus, it suggests that both the excess free polymers and β-phase are spatially far from the SWNT surfaces and are unable to efficiently transfer energy to SWNTs.

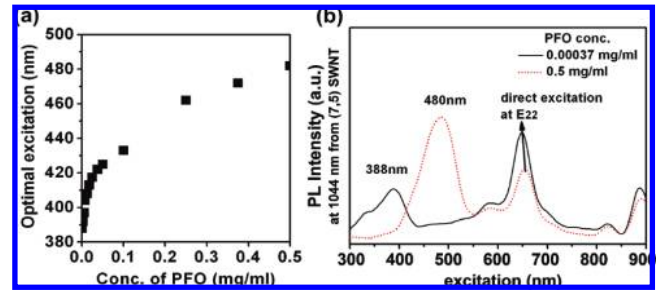

Figure 3. (a) Optimal excitation wavelength vs concentration of the excess PFO polymer. (b) The PL intensity from (7,5) SWNT monitored at 1044 nm in the PFO-SWNT(0) and PFO-SWNT(0)+PFO (0.5 mg/mL).

The PL spectrum for the PFO-SWNT+PFO (0.5 mg/mL) solution excited at 480 nm (Figure 2e) exhibits strong emission from the PFO polymers, which is in clear contrast to the absence of fluorescence either for pure PFO polymer solution (Figure S2) or PFO-SWNT solution without excess PFO (Figure 2d) upon 480 nm excitation. Moreover, a broad but weak absorption peak (~480 nm) for this solution is also revealed in Figure 2e. The optical signatures and the energy transfer phenomenon

TABLE 1: Measured NIR Emission Intensity for Each SWNT Species in PFO-SWNT(0) and PFO-SWNT(0)+PFO (0.5 mg/mL) Solutions[a]

PFO-SWNT in Toluene

SWNT species	PL-E_{22} PL intensity (a.u.) excitation through E_{22} absorption of each species	PL-388 PL intensity-388 (a.u.) Excited at 388 nm (through energy transfer)	ratio (PL-388/ PL-E_{22})
(6,5)	76.2	48.6	0.64
(7,5)	935.8	453.0	0.48
(7,6)	304.0	198.5	0.65
(8,6)	194.0	139.9	0.72
(8,7)	186.0	151.7	0.82

PFO-SWNT+PFO (0.5 mg/mL) in Toluene

SWNT species	PL-E_{22} PL intensity (a.u.) excitation through E_{22} absorption of each species	PL-480 PL intensity-480 (a.u.) Excited at 480 nm (through energy transfer)	ratio (PL-480/ PL-E_{22})
(6,5)	264.0	529.1	2.00
(7,5)	632.7	1058.8	1.67
(7,6)	286.6	432.3	1.51
(8,6)	166.9	352.3	2.11
(8,7)	269.2	406.8	1.51

[a] The PL intensity was obtained from the PLE mapping of Figure 1, panels b and c, respectively.

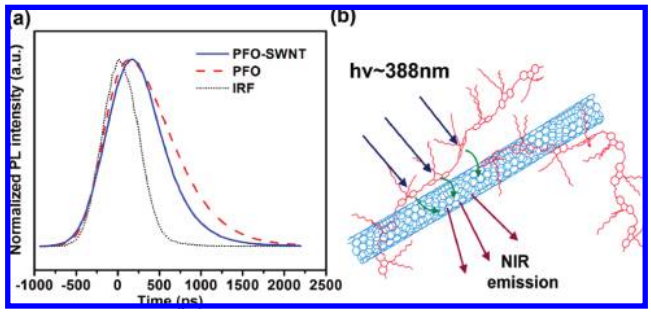

Figure 4. (a) PL lifetime profiles for PFO polymers in the presence and absence of SWNTs. (b) Schematic illustrations of energy transfer process from PFO to SWNTs.

associated with the 480 nm absorption indicate the presence of a more extended PFO conformation. Owing to the general belief that energy transfer between two chromophores are normally in close proximity (<10 nm),[31] the extended PFO structure associated with the 480 nm absorption is suggested to be in close proximity to SWNT surfaces. In fact, the optimal PFO excitation wavelength for causing NIR emissions from SWNTs can be tuned from 388 to 480 nm depending on the concentration of excess PFO polymers, as demonstrated in Figure 3a. It has been reported that the $\pi-\pi$ interaction between conjugated polymers and SWNTs usually results in band broadening or shift of the polymer's absorption peak due to the change of effective conjugation length.[32−34] Therefore, our result suggests that the conformation of the PFO polymers closely proximate to SWNT surfaces becomes more extended with the addition of excess PFO polymers. The SWNT surface provides a platform to enhance the aggregation of PFO and the driving force of polymer conformation extension is attributed to the concentration of PFO polymer. The result also suggests that the free PFO polymer is in a dynamic equilibrium[35] with the PFO polymer proximate to SWNT surfaces. Moreover, Wallace et al. have also shown that the surfactant structure around SWNTs was concentration dependent, which also favors the viewpoint of dynamic arrangement of molecules on SWNT surfaces.[36]

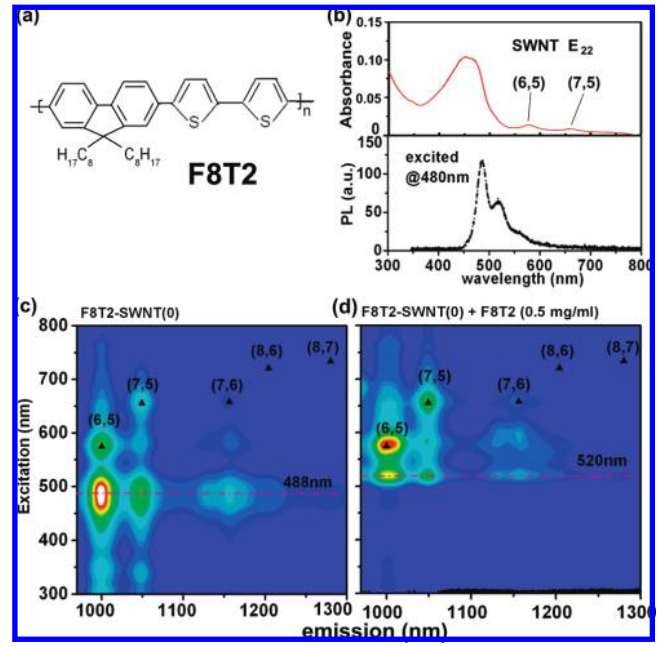

Figure 5. (a) Chemical structure of F8T2. (b) Absorption and PL spectra (excited at 480 nm) for the F8T2-SWNT hybrid in toluene. (c) PLE mapping for the F8T2-SWNT hybrid in toluene, where seven major SWNT species (6,5), (7,5), (7,6), (8,6), and (8,7) are identified. The concentration of F8T2 polymer is 0.0016 mg/mL. (d) The PLE mapping for the F8T2-SWNT +0.5 mg/mL of F8T2. It is observed that the optimal excitation wavelength for the F8T2-SWNT solution is shifted from 480 to 520 nm by adding excess (0.5 mg/mL) F8T2 polymers.

To illustrate the effect of polymer concentration on PL changes, we take the (7,5) SWNT species as an example and plot its excitation spectrum: the PL emission intensity at 1044 nm (the NIR emission peak for (7,5) SWNT) as a function of excitation wavelength. Figure 3b shows the excitation spectra for the (7,5) SWNT species existed in two extreme samples: (1) PFO-SWNT(0) (with 0.00037 mg/mL of PFO) and (2) with 0.5 mg/mL of excess PFO polymers, where the PL intensity are normalized by the power of light source at each excitation wavelength. It is observed that not only the optimal excitation wavelength shifts from 388 to 480 nm but also the PL intensity increases with the addition of excess PFO polymers. From Figure 3c, we can obtain the ratio (~0.48) of the PL intensity excited at the optimal absorption wavelength (388 nm) to its PL intensity excited through the E_{22} absorption of SWNTs in PFO-SWNT(0). The ratio for PFO-SWNT(0)+PFO(0.5 mg/mL); the PL intensity excited at the optimal absorption wavelength (480 nm) to its PL intensity through E_{22} excitation is around 1.67. The ratio indicates the relative energy transfer efficiency normalized by the content of each SWNT species. We summarize in Table 1 that the ratio for various SWNT species in PFO-SWNT(0)+PFO (~1.51 to 2.11) is higher than that in PFO-SWNT(0) (~0.48 to 0.82). This result also postulates that increasing the polymer concentration is an efficient method of enhancing the NIR emissions from SWNTs.

The precise organization of PFO polymers on SWNTs is not yet clear and worth more investigations. Nevertheless, a recent report has pointed out the possibility of the formation of regular PFO packing on SWNT surfaces,[35] and the process is suggested to be dynamic (depending on the polymer concentration). The packing of polymer chain on SWNT surfaces induced by strong $\pi-\pi$ interaction (between aromatic polymer and SWNT) is likely the root cause for the extension of conjugation length. And this model well explains the shift of the optimal excitation

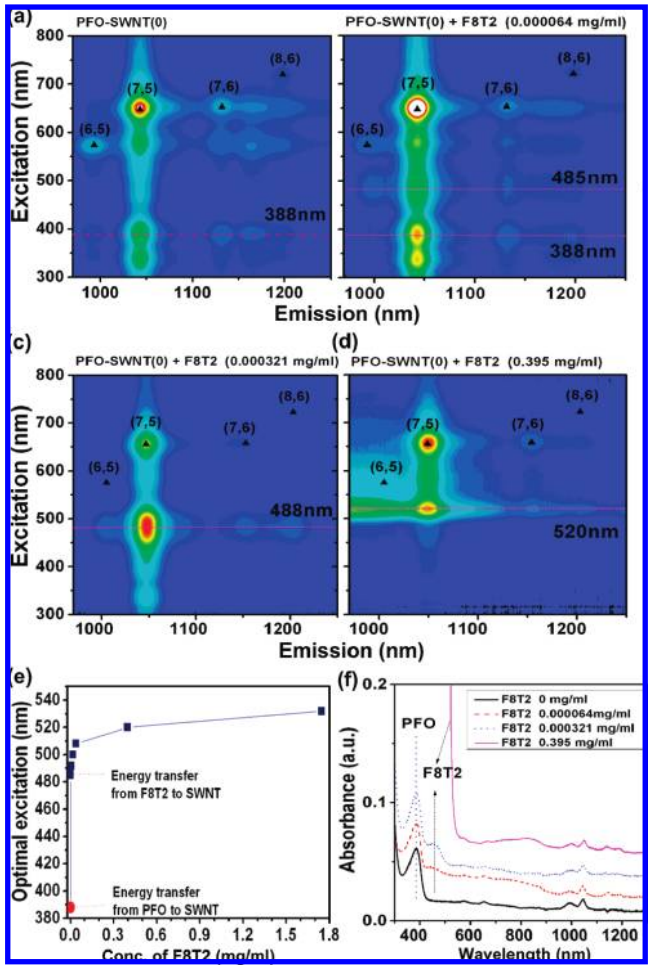

Figure 6. PLE mappings for (a) PFO-SWNT(0), (b) PFO-SWNT(0)+F8T2 (0.000064 mg/mL), (c) PFO-SWNT(0)+F8T2 (0.000321 mg/mL), and (d) PFO-SWNT(0)+F8T2 (0.395 mg/mL). (e) Optimal excitation wavelength vs concentration of the excess F8T2 polymer in PFO-SWNT(0). Noted the PFO concentration in the solution is 5.7×10^{-4} mg/mL. (f) Optical absorbance for PFO-SWNT(0) added with various concentrations of F8T2 polymers as indicated.

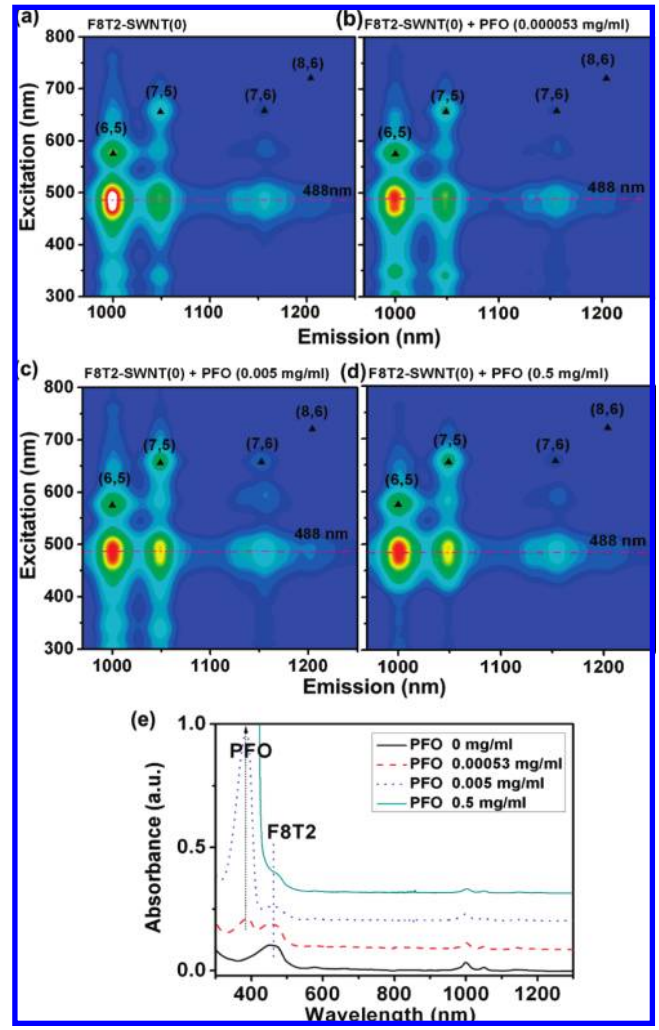

Figure 7. PLE mappings for (a) F8T2-SWNT(0), (b) F8T2-SWNT(0)+PFO (0.00053 mg/mL), (c) F8T2-SWNT(0)+PFO (0.005 mg/mL), and (d) F8T2-SWNT(0)+PFO (0.5 mg/mL). (e) Optical absorbance for F8T2-SWNT(0) added with various concentrations of F8T2 polymers as indicated. Noted the F8T2 concentration in the solution is 0.0016 mg/mL.

wavelength observed in this work. Moreover, the strategy by organizing flavin mononucleotide onto SWNT surface through $\pi-\pi$ interaction has been successfully adopted to selectively wrap around certain SWNT species,[37] which arguments also lend strong supports to the conclusion drawn from our PLE measurement.

Supporting Evidence from Fluorescnece Lifetime Measurements. To support the argument of energy transfer from PFO polymers to SWNTs, PL lifetimes of PFO in the absence and presence of SWNTs were measured using time-resolved PL spectroscopy (Figure 4a). The IRF peak position is defined as time $t = 0$ for the convenience of reading. And the PL lifetime for each solution is determined by the fitting procedure described in the experimental section. It is observed that the pure PFO polymers in solution exhibits a PL lifetime of 555 ps and the PFO polymers in PFO-SWNT(0) shows a shortened lifetime (~395 ps). The lifetime shortening of PFO suggests the occurrence of Forster resonance energy-transfer from PFO to SWNTs.[38] Figure 4b schematically illustrates the energy transfer process from PFO to SWNTs in the solution PFO-SWNT(0).

Energy Transfer from F8T2 to SWNTs. We have comparatively performed the energy transfer study for (F8T2; chemical structure shown in Figure 5a). The result suggests that the optimal excitation wavelength for F8T2-SWNT system is

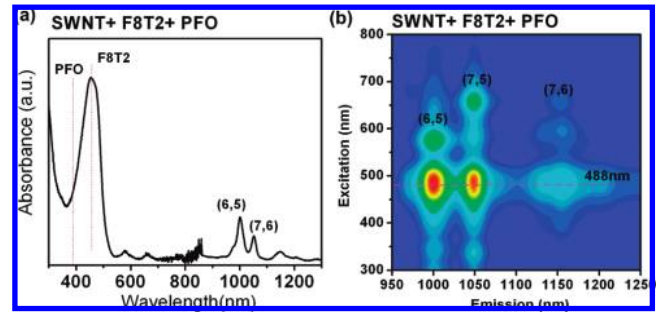

Figure 8. (a) Optical absorbance and (b) PLE mapping for the SWNT+F8T2+PFO. The preparation of the sample is described in the text.

also tunable, similar to previously observed for PFO-SWNT system. Figure 5c shows the PLE mapping for the F8T2-SWNT hybrid thoroughly washed with and redispersed in fresh toluene (F8T2-SWNT(0)), where the concentration of F8T2 was 0.0016 mg/mL and five major SWNT species (6,5), (7,5), (7,6), (8,6), and (8,7) are identified in PLE map. The absorption peak of F8T2 polymer in Figure 5b is relatively broader (450−490 nm) and the optimal excitation wavelength for SWNT emissions, centered at ~480 nm, matches well with its absorption. Figure

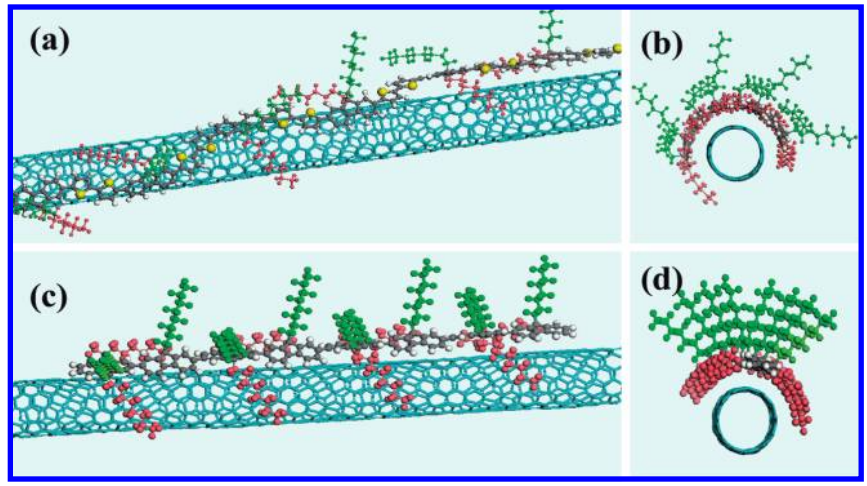

Figure 9. Optimized structure of (a and b) F8T2-SWNT and (c and d) PFO-SWNT based on molecular simulations. The sulfur atoms within F8T2 are high-lighted in yellow. To demonstrate the effects of alkyl side chains, the side chains wrapping on the SWNT are colored in red and others are in green.

5d shows the PLE mapping for the F8T2-SWNT(0) +0.5 mg/mL of F8T2. It is observed that the optimal excitation wavelength for the F8T2-SWNT solution is shifted from 480 to 520 nm by adding excess (0.5 mg/mL) F8T2 polymers.

Binding Competition between PFO and F8T2. The energy transfer from photoactive polymers to SWNTs as explored by PLE measurements can be used to study the SWNT binding competition between two polymers, PFO and F8T2. First, we dispersed the SWNTs with PFO in toluene and obtained a fresh PFO-SWNT(0) solution in which the PFO concentration was estimated to be 5.7×10^{-4} mg/mL. Five major species were identified in its PLE mapping as shown in Figure 6a, where the optimal excitation wavelength to cause the energy transfer from PFO to SWNTs was at around 388 nm. Figure 6, panels b and c, shows the PLE mapping for the solution after adding increasing amounts of F8T2 polymers. Figure 6f shows the optical absorption spectra for these solutions. After the addition of very small amount (6.4×10^{-5} mg/mL) of F8T2, the presence of emissions from SWNTs caused by 485 nm excitation in PLE map (Figure 6b) is attributed to the energy transfer from F8T2 polymers to SWNTs. This suggests that F8T2 polymers approach SWNT surfaces to enable the energy transfer to SWNTs. It is noted that after addition of excess F8T2 polymers we performed a short period (3 min) of tip-sonication to help to energize the mixing of polymers and SWNTs. Therefore the F8T2 polymers shall be able to bind with SWNTs if the F8T2-SWNT complex is energetically favorable. Figure 6c shows the PLE mapping obtained after the F8T2 polymer reaches a higher concentration (3.21×10^{-4} mg/mL). It is observed that the energy transfer for F8T2 to SWNT (optimal excitation at 488 nm) is dominant and the emissions caused by PFO energy transfer (excited at 388 nm) disappear. It is noteworthy pointing out that the concentration of P8T2 is still lower than that of PFO in this solution. Therefore, the observed preference of energy transfer from F8T2 to SWNTs may suggest that F8T2 forms relatively stable complex with SWNTs compared with PFO. Figure 6d shows the PLE mapping for the solution reaching a very high concentration (0.395 mg/mL) of F8T2 and the optimal excitation wavelength is significantly red-shifted to around 520 nm. We plot the optimal excitation wavelength for the energy transfer process from F8T2 to SWNTs as a function of the concentration of F8T2 polymers in Figure 6e. The red-shifting of optimal excitation wavelength with the polymer concentration is the same as the observation for F8T2-SWNT+F8T2 in Figure 5, where the polymer concentration of the F8T2 polymers proximate to SWNT surfaces is more extended with increasing F8T2 concentration. The result strongly indicates that SWNTs are preferentially bound with by F8T2 polymers.

A comparative experiment has also been performed to further explore the SWNT binding preference with F8T2 polymers. We dispersed the SWNTs with F8T2 in toluene and obtained a fresh F8T2+SWNT(0) solution, where the concentration of F8T2 was around 0.0016 mg/mL. The PLE measurements were performed for the solution before and after adding increasing concentrations of PFO polymers (Figures 7a−7d). The optical absorption spectra for these solutions are also shown in Figure 8e. The optimal excitation wavelength for all the solutions is unchanged (at around 488 nm), regardless of the concentration of the added PFO polymers (0.00053, 0.005, and 0.5 mg/mL). If the PFO polymer is able to approach SWNT surfaces and transfer the energy to SWNT, the emissions of SWNTs caused by PFO shall be expected in PLE. Based on Figure 3a, the optimal excitation energy for SWNTs with the PFO concentration of 0.00053 or 0.005 mg/mL should be found in between 388 and 400 nm. In other words, we expect to see obvious PLE peaks in Figure 7, panels b and c, when the excitation is in between 388 and 400 nm. However, the all PLE maps show only the signature of energy transfer from F8T2 to SWNT but no contribution from PFO is identified. This absence of energy transfer from PFO to SWNTs strongly suggests that the F8T2 polymers securely wrap the SWNTs, and the PFO polymers are likely rejected from SWNT surfaces. The result corroborates that SWNTs preferentially bind with F8T2 polymers.

To further examine the preferential binding of F8T2 with SWNTs, we disperse SWNTs with F8T2 and PFO by mixing 8 mg of CoMoCat with 10 mg of PFO and 10 mg of F8T2. After sonication, centrifugation, filtration and rigorous washing, the SWNT-polymer hybrids on the filter paper were redispersed in toluene (SWNT+PFO+F8T2) for optical measurements. The absorption spectra in Figure 8a and the PLE map in Figure 8b consistently demonstrate that PFO polymers are washed off and only F8T2 polymers are left, indicating that F8T2 polymers strongly bind with SWNTs.

Result of Molecular Modeling. We have tested several model systems consisting of F8T2 and PFO polymers with different length and the details of the binding energies are tabulated in the Supporting Information. Figure 9 demonstrates

the optimized chemical structures for F8T2-SWNT and PFO-SWNT hybrids based on molecular simulations. We found that regardless of the length of the polymer, the average distance between the backbone of the aromatic polymers and SWNT is around 3.4 Å indicating the stronger interaction between them. The binding energy of F8T2 and SWNT is systematically higher than that of PFO by ~16 kcal/mol per unit. Furthermore, we have tested the effect of the side chains, while each side chain when wrapping around the SWNT provides additional binding energy of ~11 kcal/mol, they do not contribute to the preference of F8T2. It is clear from our comparisons that the energetic difference between the adsorption of F8T2 and PFO originates from the strong interaction between the 5-membered rings containing a sulfur atom on F8T2.

Conclusions

In summary, polymer concentration governs the polymer aggregation on SWNTs, which in turn controls the energy transfer and optimal excitation wavelength. The behavior is not unique to PFO or F8T2, we also observe the same phenomenon for other polymers. The energy transfer process is also useful for characterizing the nanotube binding competition between different polymers. We also point out that the optical behaviors of the polymer−SWNT composite are dominated at the interface if the phenomena are associated with the interfacial interaction. This study not only provides the understanding of energy transfer process between photoactive polymers and SWNTs, but also suggests a convenient method of adjusting the desired optical wavelengths for the energy conversion. The adjustable optimal excitation wavelength and the enhanced emissions from SWNTs are useful for polymer−SWNT composites in optoelectronic applications.

Acknowledgment. This research was supported by Nanyang Technological University, Singapore. We also thanks the financial support from National Research Foundation Singapore (NRF-CRP 2-2007-02) and National Natural Science Foundation of China (NSFC 20825314).

Supporting Information Available: Additional experimental information and additional figures and a table. This material is available free of charge via the Internet at http://pubs.acs.org.

References and Notes

(1) Hoertz, P. G.; Mallouk, T. E. *Inorg. Chem.* **2005**, *44*, 6828.
(2) Kymakis, E.; Amaratunga, G. A. J. *Appl. Phys. Lett.* **2002**, *80*, 112.
(3) Kymakis, E.; Amaratunga, G. A. J. *Rev. Adv. Mater. Sci.* **2005**, *10*, 300.
(4) Shi, Y.; Tantang, H.; Lee, C. W.; Weng, C. H.; Dong, X.; Chen, P.; Li, L. J. *Appl. Phys. Lett.* **2008**, *92*, 113310.
(5) Kazaoui, S.; Minami, N.; Nalini, B.; Kim, Y. *J. Appl. Phys.* **2005**, *98*, 084314.
(6) Shi, Y.; Du, D.; Marsh, D. H.; Rance, G. A.; Khlobystov, A. N.; Li, L. J. *J. Phys. Chem. C* **2008**, *112*, 13004.
(7) Star, A.; Lu, Y.; Bradley, K.; Gruner, G. *Nano Lett.* **2004**, *4*, 1587–1591.
(8) Shi, Y.; Dong, X.; Tantang, H.; Chen, F.; Lee, C.; Zhang, K.; Chen, Y.; Wang, J.; Li, L. J. *J. Phys. Chem. C* **2008**, *112*, 18201.
(9) Borghetti, J.; Derycke, V.; Lenfant, S.; Chenevier, P.; Filoramo, A.; Goffman, M.; Vuillaume, D.; Bourgoin, J. P. *Adv. Mater.* **2006**, *18*, 2535.
(10) O'Connell, M. J.; Bachilo, S. M.; Huffman, C. B.; Moore, V. C.; Strano, M. S.; Haroz, E. H.; Rialon, K. L.; Boul, P. J.; Noon, W. H.; Kittrell, C.; Ma, J. P.; Hauge, R. H.; Weisman, R. B.; Smalley, R. E. *Science* **2002**, *297*, 593.
(11) Chen, R. J.; Zhang, Y. G.; Wang, D. W.; Dai, H. J. *J. Am. Chem. Soc.* **2001**, *123*, 3838.
(12) Cherukuri, P.; Bachilo, S. M.; Litovsky, S. H.; Weisman, R. B. *J. Am. Chem. Soc.* **2004**, *126*, 15638.
(13) Wang, R. K.; Chen, W. C.; Campos, D. K.; Ziegler, K. J. *J. Am. Chem. Soc.* **2008**, *130*, 16330.
(14) Umeyama, T.; Kadota, N.; Tezuka, N.; Matano, Y.; Imahori, H. *Chem. Phys. Lett.* **2007**, *444*, 263.
(15) Nish, A.; Hwang, J. Y.; Doig, J.; Nicholas, R. J. *Nanotechnology* **2008**, *19*, 095603.
(16) Chen, F.; Wang, B.; Chen, Y.; Li, L. J. *Nano lett.* **2007**, *7*, 3013.
(17) Cheng, F.; Imin, P.; Maunders, C.; Botton, G.; Adronov, A. *Macromolecules* **2008**, *41*, 2304.
(18) Hasan, T.; Tan, P. H.; Bonaccorso, F.; Rozhin, A. G.; Scardaci, V.; Milne, W. I.; Ferrari, A. C. *J. Phys. Chem. C* **2008**, *112*, 20227.
(19) Hasan, T.; Scardaci, V.; Tan, P. H.; Rozhin, A. G.; Milne, W. I.; Ferrari, A. C. *Physica E* **2008**, *40*, 2414.
(20) Star, A.; Stoddart, J. F. *Macromolecules* **2002**, *35*, 7516.
(21) Izard, N.; Kazaoui, S.; Hata, K.; Okazaki, T.; Saito, T.; Iijima, S.; Minami, M. *Appl. Phys. Lett.* **2008**, *92*, 243112.
(22) MS: Cerius 2 Software, Accelrys Inc., Nanyang Technology University, School of Materials Science and Engineering.
(23) Rappé, A. K.; Casewit, C. J.; Colwell, K. S.; Goddard, W. A.; Skiff, W. M. *J. Am. Chem. Soc.* **1992**, *114*, 10024.
(24) Lebedkin, S.; Hennrich, F.; Koiwski, O.; Kappes, M. M. *Phys. Rev. B.* **2008**, *77*, 165429.
(25) Miyaichi, Y.; Maruyama, S. *Phys. Rev. B* **2006**, *74*, 035415.
(26) Tan, P. H.; Rozhin, A. G.; Hasan, T.; Hu, P.; Scardaci, V.; Milne, W. I.; Ferrari, A. *Phys. Rev. Lett.* **2007**, *99*, 137402.
(27) Lebedkin, S.; Arnold, K.; Hennrich, F.; Krupke, R.; Renker, B.; Kappes, M. M. *New J. Phys.* **2003**, *5*, 140.1.
(28) Strano, M. S.; Doom, S. K.; Haroz, E. H.; Kittrell, C.; Hauge, R. H.; Smalley, R. E. *Nano Lett.* **2003**, *3*, 1091.
(29) Cadby, A. J.; Lane, P. A.; Wohlgenannt, M.; An, C.; Vardeny, Z. V.; Bradley, D. D. C. *Synth. Met.* **2000**, *111*, 515.
(30) Kitts, C. C.; Bout, D. A. V. *Polymer* **2007**, *48*, 2322.
(31) Joseph, R. L. *Principles of Fluorescence Spectroscopy*, 2nd ed.; Plenum Publishing Corporation: New York, 1999.
(32) Chen, J.; Liu, H.; Weimer, W. A.; Halls, M. D.; Waldeck, D. H.; Walker, G. C. *J. Am. Chem. Soc.* **2002**, *124*, 9034.
(33) Star, A.; Stoddart, J. F.; Steuerman, D.; Diehl, M.; Boukai, A.; Wong, E. W.; Yang, X.; Chung, S. W.; Choi, H.; Heath, J. R. *Angew. Chem., Int. Ed.* **2001**, *40*, 1721.
(34) Geng, J.; Kong, B. S.; Yang, S. B.; Youn, S. C.; Park, S.; Joo, T.; Jung, H. T. *Adv. Func. Mater.* **2008**, *18*, 2659.
(35) Papadimitrakopoulos, F.; Ju, S. Y. *Nature* **2007**, *450*, 486.
(36) Wallace, E. J.; Sansom, M. S. P. *Nano Lett.* **2007**, *7*, 1923.
(37) Ju, S. Y.; Doll, J.; Sharma, I.; Papadimitrakopoulos, F. *Nat. Nanotechnol.* **2008**, *3*, 356.
(38) Biju, V.; Itoh, T.; Baba, Y.; Ishikawa, M. *J. Phys. Chem.* **2006**, *110*, 26068.

JP904431U